Fast Initiation of Peptide and Protein Folding Processes

Martin Volk[a]

Keywords: Amino acids / Helical structures / Kinetics / Photochemistry / Protein folding

The investigation of fast processes of peptide and protein folding has received increasing attention in the last years, driven by the development of new experimental approaches that make it possible to go beyond the millisecond time resolution of standard stopped-flow or rapid mixing techniques. The new methods allow the direct observation of important first steps such as hydrophobic collapse or secondary structure formation during the transition from the disordered polypeptide to the functional protein. However, most of these techniques are limited to a very narrow range of proteins or have other experimental restrictions and shortcomings. This review, after an overview and discussion of previously employed methods, describes a novel fast optical trigger for protein folding. This optical trigger has the potential to be used in the study of a wide variety of proteins and peptides without any of the restrictions of previous approaches. In an initial application of this technique, α-helix folding in short peptides was investigated.

Introduction

The question of how peptides or proteins fold to produce their unique and highly organised functional three-dimensional structures is one of the most challenging questions currently being investigated in biological research. An unfolded polypeptide with a specific primary sequence of amino acids folds into a well-defined three-dimensional structure, which is the basis of the biological or catalytic function of the folded protein or peptide. At least for small proteins, this process is fully reversible and does not rely on external assistance.[1] Therefore, the native structure is expected to correspond to the conformation of lowest Gibbs free energy and should be determined solely by the amino acid sequence along the polypeptide backbone ("thermodynamic hypothesis"[1]). In recent years, there has been an increasing interest in the prediction of protein structure from the primary sequence,[2] boosted in particular by the growing field of rational design of new peptides[3] with highly interesting new medical or industrial applications and more recently by the availability of the complete human genome.

The investigation of the *dynamic* aspects of the folding process is important for elucidation of the detailed mechanism(s) by which protein folding proceeds. As originally pointed out by Levinthal, a purely random search of all possible conformations of a protein would not be able to find the native structure on physiological timescales,[4] and protein folding must therefore be a highly directed process. Several partly conflicting models have been proposed to describe this process and the underlying mechanism directing it towards the native structure. These include the framework or diffusion-collision model,[5–7] the hydrophobic collapse model[8–10] and the nucleation-condensation model[11,12] (see Figure 1). Only more detailed experimental information on the nature of the earliest steps of protein folding will allow us to distinguish between these models. A comparison of the timescales for the initial collapse of an extended unfolded polypeptide and for the formation of secondary structure, for example, would be an important step

[a] Surface Science Research Centre, University of Liverpool, Liverpool L69 3BX, United Kingdom
Fax: (internat.) + 44-151/708-0662
E-mail: m.volk@liverpool.ac.uk

Martin Volk, born in 1960, studied physics at the Technical University of Munich (Germany), where he obtained his Diploma in 1986 and received his Ph.D. in 1991 for nanosecond time-resolved spectroscopic studies on photosynthetic reaction centres under the supervision of Prof. M. E. Michel-Beyerle at the Institute of Physical Chemistry. After post-doctoral work in Munich and with Prof. R. M. Hochstrasser at the University of Philadelphia (USA), he took up his current position as Lecturer at the Surface Science Research Centre at the University of Liverpool (UK) in 1999. His research interests focus on the application of fast and ultrafast time-resolved spectroscopy to the investigation of a large variety of chemical and biological processes, including reaction dynamics at metal surfaces and electrochemical interfaces, electron transfer in proteins and model systems and fast processes of protein folding.

MICROREVIEWS: This feature introduces the readers to the authors' research through a concise overview of the selected topic. Reference to important work from others in the field is included.

  1434–193X/01/0714–2605 $ 17.50+.50/0

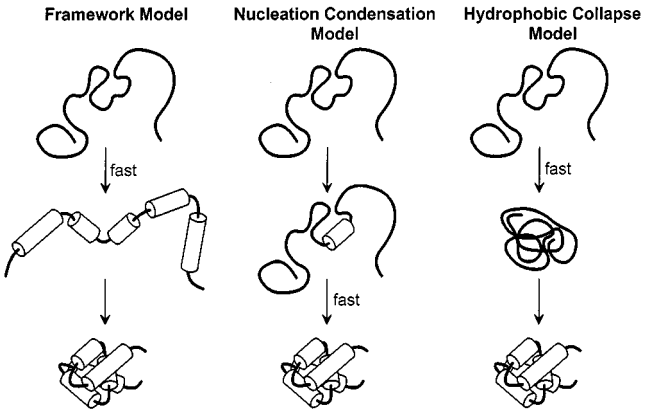

Figure 1. Schematic (and highly simplified) illustration of different models for protein folding. Thick lines indicate disordered polypeptide, columns represent peptide segments with well-defined secondary structure, such as α-helices. In the *framework* model, some peptide segments adopt their native secondary structure before being packed together to form the final three-dimensional protein; the initially formed segments with secondary structures are assumed to be stable, as shown here. In the closely related *diffusion-collision* model (not shown) segments with secondary structure are thought to diffuse together in the same way; in this model, however, the segments with secondary structure are highly unstable and are present in the unfolded peptide with only low probabilities, stabilising each other only when coming into contact. The *nucleation-condensation* model assumes the rate-limiting step to be the formation of a small nucleus of the final structure, which provides a template for fast folding of the rest of the protein. The *hydrophobic collapse* model suggests a fast collapse of the unfolded protein, driven by the hydrophobic effect, resulting in a more or less disordered compact state with hydrophobic residues in the inside and hydrophilic residues on the outside; secondary structure and tertiary contacts are then formed within this compact aggregate on a shorter timescale.

towards the distinction between framework and hydrophobic collapse model.

On the other hand, dynamic aspects of protein folding are also of great relevance in the context of the prediction of the final structure of rationally designed proteins or peptides. Both natural proteins and designed peptides will only adopt the anticipated (lowest free-energy) structure on a reasonable timescale if there is an efficient folding pathway guiding the polypeptide towards this structure and avoiding the accumulation of metastable nonfunctional folds or traps. Of particular (although not exclusive) concern here are disulfide cross-links between cysteines, which can result in stable kinetic traps. The formation of nonnative disulfide bonds or the stabilisation of a nonnative fold by a prematurely formed native disulfide bond may inhibit − or at least significantly retard − the folding to the native structure, as exemplified by the complex oxidative folding pathway of bovine pancreatic trypsin inhibitor (BPTI).[7,13] On the other hand, disulfide bonds can only be formed if the motion of the polypeptide backbone brings two cysteine groups into close contact during the early folding stages. Thus, a detailed understanding of the interplay between peptide backbone folding and disulfide bond formation is important for the correct prediction of the folding pathway of any natural or designed protein. In the long term, it may even become possible to implement an efficient folding pathway in the peptide design, possibly making use of some of nature's tricks, such as the prosequences that enhance the folding dynamics of BPTI[14] or subtilisin.[15]

Dynamic aspects of protein folding, and of secondary structure formation in particular, may also be important for elucidation of the molecular mechanisms behind conditions such as the amyloid diseases (including Alzheimer's and the prion diseases). These diseases are characterised by a change in protein conformation, typically involving major secondary structural changes that result in pathological deposits in the infected cells.[16]

It is often assumed that the initial rapid phase of protein folding, the collapse from the fully unfolded polypeptide to a more compact form, involves the formation of secondary structural elements such as α-helices, β-strands or β-turns, thus significantly narrowing the conformational space that the protein has to explore in the search for the lowest free-energy state.[6,7,9,12,17] Regions with secondary structure may then act as nucleation sites for the further collapse to the final native state. In many cases, the formation of native structural elements has been observed to occur during a "burst phase" within the dead time of the measurement, on timescales of less than a millisecond after the initiation of protein folding.[18] Theoretical studies have also suggested fast folding times. Thus, α-helix formation was predicted to occur on the 10-ns timescale by combining the Zimm−Bragg model[19] and explicit simulations of the thermodynamic barrier associated with helix initiation and propagation.[20] Molecular dynamics simulations have suggested protein conformational changes on the timescale of picoseconds and nanoseconds.[21] These timescales are much too short for most of the experimental investigations performed to date, which were based on rapid-mixing or stopped-flow techniques. In these experiments the protein is prepared under unfolding solution conditions (such as high concentrations of denaturants or unfavourable pH values). The folding process is then induced by a sudden change in these conditions, brought about by rapid mixing with other suitable solutions. The time resolution of such methods is limited by the time required for efficient mixing, which in standard setups is of the order of milliseconds and which even with highly sophisticated techniques could not be reduced to below 40 μs.[22−24] Clearly, more specialised techniques are needed for initiation ("triggering") of the fastest processes of protein folding and secondary structure formation.

This review discusses experimental approaches for the investigation of early protein-folding processes. It is divided into three parts: (i) a short summary of the techniques used for *observing* fast peptide and protein folding processes; (ii) an overview of methods used previously for *triggering* the folding of peptides or proteins on short timescales; and (iii) a description of a recently developed novel optical trigger mechanism, based on a synthetic amino acid which is used for the formation of a structure-distorting aryl disulfide cross-link; this aryl disulfide bond can be broken by ultrafast photodissociation, which allows one to start the folding process on the subpicosecond timescale.

It will be seen that in recent years some innovative approaches have been very successful in providing initial insights into the fastest processes of peptide and protein folding. However, most of the techniques for initiating folding on the short timescales available at present are restricted to particular proteins or can only be applied under certain (often nonphysiological) conditions; so new approaches need to be developed. Most probably, significant progress in this field will only be achieved by concerted efforts from a broad range of disciplines. These need to include not only the biologists and biophysicists who have traditionally worked on the problem of protein folding, but the example of the disulfide bond photo trigger mechanism clearly shows, organic chemists can also make significant contributions to the field of protein folding, and their help with tackling this "old" problem is urgently needed.

Techniques for the Observation of Fast Folding Processes in Real-Time

A number of experimental approaches are available for the real-time observation of peptide or protein folding processes on short timescales (nanoseconds or shorter). Some of these methods monitor highly localised structural changes, whereas others are better suited for the observation of global folding dynamics or overall secondary structural changes. Different techniques can thus yield complementary information and the simultaneous use of several techniques often significantly enhances the conclusions which can be drawn from a particular experiment.

Absorbance

The absorbance bands of prosthetic groups are usually sensitive to local environmental changes. The transfer of a chromophore from the polar aqueous solution into the nonpolar protein interior is expected to shift the position of its absorbance bands, as are protein rearrangements which change the chromophore's proximity to specific (e.g. polar) amino acid residues. One prominent example is the absorbance of the cofactor of heme proteins in the Soret (400−420 nm) or visible region, which has been widely used to follow the collapse of such proteins from the unfolded structure and to monitor more specific ligand-binding processes during the formation of the final structure.[25−33]

Fluorescence Methods

Fluorescence methods can provide a wide range of protein structural and dynamic information, depending on the nature of the fluorophore, the presence of fluorescence quenchers and the particular fluorescence property being measured (such as yield, lifetime, anisotropy or spectral characteristics).[34] Particularly useful for fluorescence studies on proteins are their aromatic amino acid residues, which function as intrinsic probes, avoiding any distortion of the protein. Alternatively, extrinsic fluorescence probes can be bound to the peptide covalently or attached noncovalently.

Fluorescence methods can be used to observe both local and global structural changes on short timescales. Spectral characteristics, in particular the wavelength of the fluorescence maximum, are highly sensitive to the fluorophore's surroundings. Like absorbance bands, the fluorescence spectrum will shift upon folding from the random conformation, which exposes the probe to the polar aqueous solvent, to a more compact structure with the probe buried inside the hydrophobic protein core. Such spectrally resolved and integrated measurements have been used to observe protein collapse dynamics and to draw conclusions about the solvent exposure of tryptophan in different kinetic intermediates during protein folding.[35,36]

Fluorescence quenching, measured either by the overall fluorescence yield or by time-resolved observation of the fluorescence decay after a short laser flash, can yield even more detailed information. Again, experiments of this type can be designed to observe either global or local structural changes. Addition of an extrinsic fluorescence quencher that cannot access the fluorophore when it is buried inside the folded protein, for example, can yield information on global folding or collapse dynamics.[37,38] On the other hand, the fluorescence of an energy donor D can be quenched by an energy acceptor A by distance-dependent, nonradiative excitation energy transfer.[39] Time-resolved observation of the fluorescence yield or fluorescence lifetime gives direct information on the time dependence of the distance between D and A and thus information on the relative motion of different parts of the protein (see Figure 2). Like the fluorophore itself, the energy acceptor may be an extrinsic or intrinsic chromophore. In particular, the quenching of tryptophan fluorescence by the heme cofactor or other amino acid residues has been widely used in investigations of heme protein folding on short timescales.[22,24,37,40−45] On the other hand, covalently bound fluorophores or fluorescence quenchers have been used to observe fast folding dynamics of proteins[29,46] and synthetic peptides.[47,48]

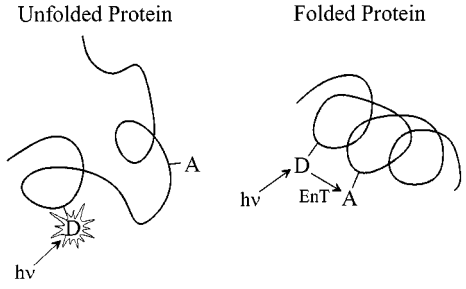

Figure 2. Schematic illustration showing how, in a folded protein, the fluorescence of energy donor D can be quenched by a suitably positioned energy acceptor A by nonradiative energy transfer (EnT), whereas the distance between D and A is too large for efficient quenching for most conformations of the unfolded protein.

Infrared Absorbance

A generally applicable method for observing secondary structural changes in proteins and peptides is provided by infrared spectroscopy. The peptide amide I mode near 1650

cm^{-1}, which mainly involves the C=O stretch vibration of the peptide backbone, is a sensitive indicator of secondary structure.[49] Upon secondary structure formation, its frequency is shifted by hydrogen bonding and transition dipole coupling, both of which depend on the relative geometry of the peptide groups.[50] Figure 3A shows that the amide I′ band[51] of a short α-helical peptide shifts to higher frequencies when the temperature is raised, causing the melting of the helix; i.e., the transition from an α-helical to a random coil structure. The existence of an isosbestic point at 1648 cm^{-1} and the shape of the difference spectra in Figure 3B show that this shift is not the product of a gradual temperature-induced shift, but of the changing relative contributions from two distinct absorbance bands: one at 1633 cm^{-1}, which dominates at low temperatures and is attributable to the α-helical structure, and one at 1658 cm^{-1}, which is more pronounced at higher temperatures and is attributable to the unfolded random coil.[52,53] Shifts of the amide I band have been used by several authors for observing fast folding or unfolding reactions in proteins[54−58] and de novo peptides.[52,56,59] Recent progress in the field of ultrafast laser technology[60] has extended the timescale of infrared measurements into the femtosecond time domain, so that even the fastest conformational changes are observable in real-time.

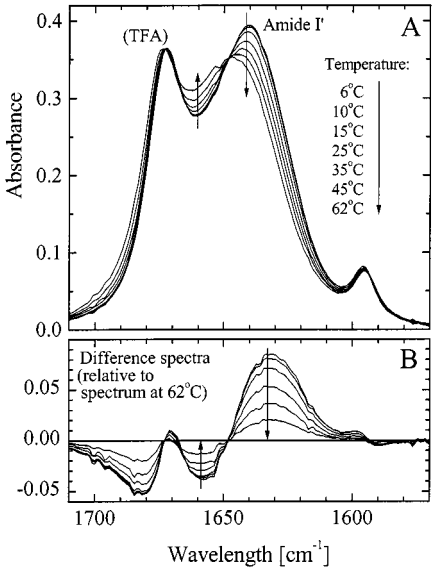

Figure 3. (A) Temperature-dependent FTIR spectra of peptide **5**, corrected for D_2O background absorbance at each temperature. The absorbance around 1675 cm^{-1} originates from the TFA counter-ion present in the solution. (B) Difference spectra, calculated by subtraction of the spectrum at 62 °C from each spectrum. Peptide concentration approximately 10 mM in D_2O, path length 56 μm.

Time-resolved amide I band IR measurements yield results relating to changes in the *overall* secondary structure content of peptides or proteins, since all peptide bonds contribute equally to the signal. Local probing (at residue level) can be achieved with the aid of isotopic labelling, such as the replacement of $^{12}C=O$ by $^{13}C=O$, which shifts the amide I band by approx. 40 cm^{-1}. Although this method has been used for the selective determination of the stability of different parts of an α-helical peptide,[53] it has not yet been used for time-resolved measurements.

Circular Dichroism

Secondary structural changes can also be observed by circular dichroism (CD) spectroscopy, which is based on the differential absorption of left- and right-circularly polarised light by a chiral chromophore. Non-time-resolved CD measurements of the amide group absorption in the 190−230-nm region have been widely used for the determination of protein and peptide secondary structures.[61] Nanosecond time-resolved CD measurements are technically challenging, but have been performed to obtain dynamic information on secondary structure formation in heme proteins,[30,62] complementing information on ligand binding processes observed by heme absorbance measurements.

Resonance Raman Scattering

Although not yet widely used for fast protein folding studies, resonance Raman techniques have the potential to observe overall secondary structure[63] (similarly to IR absorption) or local structural changes, depending on the chromophore under investigation (such as amide groups, aromatic side-chains or protein cofactors). Resonance Raman measurements have been used to determine the heme ligands in different folding intermediates of heme proteins and to provide information on the development of native tertiary structure around the heme.[23,45,64,65] In a recent investigation, resonance Raman scattering was used to follow the unfolding of a short α-helical peptide.[66]

Other Techniques

A variety of other, more specialised techniques have been shown to be useful for the investigation of particular fast protein folding processes. Magnetic circular dichroism (MCD) spectroscopy, in which optical activity is induced by the application of an external magnetic field, is particularly sensitive to the disturbance of the electronic states of a chromophore by the surrounding structure,[67] and has been used to study ligand-formation processes during the folding of cytochrome c.[68] The EPR signals of spin labels, which can be selectively attached to specific protein sites, depend on their tumbling mobility and so change upon the formation of a more compact structure. This effect has been used to measure cytochrome c folding kinetics on the 100-μs timescale.[69] Small-angle X-ray scattering experiments have been performed on cytochrome c to yield the radius of gyration of a folding intermediate on the 100-μs timescale.[70] Finally, protein volume changes upon unfolding of apomyoglobin have been observed to occur on the timescale of a few microseconds by time-resolved photoacoustic detection.[71]

Previously Used Methods for Fast Initiation of Peptide or Protein Folding

For the direct observation of any process on a short timescale, it is necessary to be able to *start* the process fast

enough; that is, within the desired time resolution. The standard methods for the initiation of protein folding or unfolding are based on rapid-mixing techniques, in which solution conditions, such as denaturant concentration or pH, are rapidly changed from unfavourable for folding to favourable (or vice versa) by mixing with other suitable solutions. Because of the finite mixing time of standard rapid mixing setups, such experiments are normally restricted to observing processes on millisecond, or longer, timescales.

Since most of the techniques for observing protein folding can be used on short timescales, the greatest handicap for extending protein folding experiments to shorter timescales is the need to start the folding reaction on the timescale of interest. Only in the last few years have new experimental approaches (reviewed in refs.[72−75]) made it possible to trigger protein folding on short timescales (arbitrarily defined here as shorter than that of standard rapid-mixing or stopped-flow techniques, and thus shorter than 1 ms), so permitting the direct observation of fast processes in the "burst-phase" of protein folding.

Relaxation Methods

Relaxation methods, such as dielectric relaxation and ultrasonic attenuation, were employed very early on to study the helix−coil transition of α-helical homopolymers, yielding relaxation times in the range of 10 ns to 10 μs.[76] More recently, ultrasonic velocimetry has indicated conformational relaxations occurring in less than 500 ns in the acidic molten globule of α-lactalbumin.[77] However, none of these experiments give direct structural information and they only allow very indirect conclusions on folding dynamics to be made.

The timescale of intrapeptide contact formation, which is one of the elementary steps of protein folding, has been investigated by triplet energy transfer between chromophores attached to opposite ends of short peptides with purely random coil structure.[78] In these equilibrium experiments, the triplet state of one chromophore is quenched upon contact formation with the chromophore at the other peptide end. The lifetime of the triplet state is thus a measure of the contact formation time, which was observed to be in the range of 10−100 ns, depending on the length of the peptide chain.

Rapid-Mixing Techniques

Rapid mixing provides a generally applicable method for triggering protein-folding reactions by the rapid reduction of the concentration of denaturants, such as guanidine hydrochloride (GuHCl) or urea, or by a sudden change in the pH of the solution to a value more favourable for the folded protein. This technique has been widely used for the investigation of protein-folding dynamics, but until recently was limited to the timescale of milliseconds because of the dead time of standard rapid-mixing setups. Only in the last few years have continuous-flow mixers with mixing times as short as 40 μs been developed with the aim of observing faster protein-folding processes.[22−24]

The folding and unfolding of horse cytochrome c after rapid mixing has been investigated in detail, making use of fluorescence detection,[22,24,42,43] resonance Raman scattering[23,45,64,65] and CD measurements.[79] Upon folding, the heme cofactor gets sufficiently close to the sole tryptophan of cytochrome c to quench its fluorescence efficiently. The tryptophan fluorescence yield was found to decay in several phases during the transition from the denatured to the native state. All of the phases could be resolved, including a fast decay − taking place exponentially with a time constant of 57 μs − during the initial collapse from the expanded conformation to a more compact state. The observation of exponential kinetics was taken to indicate that the first large-scale motion during the folding of cytochrome c represents a one-step formation of a compact state across a rate-limiting barrier, corresponding to a three-state folding model. CD measurements showed this compact state to have a maximum of 20% of the native helix content. From this compact state, the protein folds into a more native-like state (with the native methionine heme ligand and about 70% of the native helical content) on the timescale of 400−600 μs, provided that the heme is not blocked by nonnative histidine; otherwise dissociation of the histidine on the 10−100-ms timescale becomes rate-limiting.

Only a few other proteins have been investigated by ultrafast rapid mixing, none of them in as much detail as horse cytochrome c. Kinetics similar to those in horse cytochrome c have been observed after rapid denaturant dilution for the refolding of yeast cytochrome c, using the EPR signal of a cysteine-specific spin label.[69] Folding and unfolding kinetics of apomyoglobin have been induced by rapid mixing and monitored by tryptophan fluorescence measurements, revealing two distinct intermediate states and folding/unfolding time constants as short as 200 μs.[36]

These results, obtained with highly sophisticated continuous-flow rapid mixers, constitute a major breakthrough in the investigation of fast protein-folding processes. However, processes faster than several 10 μs are not at present observable by rapid-mixing techniques. Furthermore, continuous-flow mixing setups necessitate the use of large quantities of sample and thus their application will remain limited to proteins that can be easily prepared in high yields.

Photochemical Methods

The folding of cytochromes under strongly denaturing solvent conditions can be induced by fast photochemical trigger events, such as photodissociation of carbon monoxide from the heme cofactor[25] or electron transfer to the heme.[26] The first method is based on the fact that it is possible to find denaturant concentrations at which reduced cytochrome without a CO ligand remains folded, while the same protein with a CO ligand is unfolded. Under these conditions, fast photodissociation of CO − which can be achieved on the picosecond timescale − initially creates an unligated cytochrome in its unfolded form, and this then relaxes to the more stable folded structure. In a similar manner, reduced and oxidised cytochromes have signific-

antly different folding stabilities; at certain denaturant concentrations cytochromes are unfolded in the oxidised state while remaining folded in the reduced state. Electron transfer to the oxidised unfolded cytochrome, which can be induced by photoexcitation of a suitable sensitiser, then triggers the refolding process. The timescale of initiation of protein folding by this method is limited by the electron transfer time; with freely diffusing electron donors, reduction of heme in less than 1 μs has been achieved.[26] Even shorter timescales should be possible by covalently linking the sensitiser to the protein.

Upon initiation of refolding of cytochrome c by CO photodissociation, fast changes in the heme absorbance spectrum were observed,[25,28,30,80] and were interpreted as peptide chain diffusion-limited[33,80] ligation of the heme, both by the native methionine, with a rate of 1/(40 μs), and by nonnative histidines, with a rate of 1/(400 μs), accompanied by fast ligand-exchange processes. A different interpretation of these data was suggested by time-resolved MCD measurements,[68] which implied inhomogeneous heme ligation by the methionine with a time constant of 2 μs and by histidines with a time constant of 50 μs in different conformational subpopulations of the unfolded protein, followed by ligand exchange on a much longer timescale. Although these fast ligand-binding processes constitute the first steps towards the folded protein, they are not accompanied by a significant collapse of the unfolded protein, possibly because of the high denaturant concentrations needed for unfolding the CO-bound protein.[40] Similarly, heme absorbance spectra measured after the fast initiation of folding of reduced cytochrome c by electron transfer were interpreted as indicating ligand exchange processes on the 10−100 ms timescale.[29,32,62] A covalently linked dansyl moiety, the fluorescence of which is strongly quenched in the folded state, was used to confirm that the overall folding of reduced cytochrome c after electron transfer only occurs over this slow timescale.[29,46] Time-resolved CD spectroscopy on reduced cytochrome c revealed that 10−20% of the native secondary structure is formed in the first few microseconds after CO photodissociation or electron transfer, and that no further secondary structure formation takes place on a timescale shorter than 10−100 ms.[30,62] The distribution of this secondary structure over a possibly heterogeneous protein population could not be determined, but the results are compatible with complete folding of a small fraction of all proteins in a few microseconds, driven by fast native ligand formation,[68] followed by the folding of the majority of the proteins on the 10−100-ms timescale. This slow folding of the majority of the protein population is probably due to the need to escape a semistable trap state, which arises from the binding of a nonnative histidine to the heme.

Electron-transfer-initiated protein folding has been employed for a limited number of investigations on other heme proteins. For the four-helix-bundle protein cytochrome b_{562}, the formation of the fully folded structure was observed to occur with time constants in the range of 500 μs to 3 ms at GuHCl concentrations of 2−3 M; a value of 5 μs in the absence of denaturant was predicted by extrapolation.[27,31] Deoxymyoglobin was found to fold with a time constant of about 200 μs.[81]

Although ligand dissociation or electron transfer can function as fast triggers of protein-folding processes on very short timescales, and are almost ideal triggers for heme protein folding, their application is limited to these proteins and cannot easily be extended to a wider range of samples. Unfortunately, the folding dynamics of heme proteins seem to be dominated by ligand formation and exchange processes rather than by intrinsic polypeptide dynamics, which limits the conclusions that can be drawn from such experiments as far as the general protein folding problem is concerned. Both techniques also require the presence of significant amounts of denaturants, which are known to affect the dynamics of protein folding significantly.[24,26,31,65]

A more generally applicable photochemical method for the initiation of peptide or protein folding on a short timescale might be the use of photoinduced pH jumps, which can be achieved on timescales as short as 100 ps by photoexcitation of molecules with significantly different pK_a values in their ground and their excited states[82−84] or by the release of protons from photolabile caged compounds.[71] To date, this method has been used only once for the investigation of fast protein-folding processes. In this study, nanosecond pH jumps were induced by the photoinduced release of caged protons, and fast conformational changes of apomyoglobin during its transition from the native (N) to the intermediate (I) state were followed on the sub-microsecond timescale by time-resolved photoacoustic detection.[71]

Fast Temperature Jumps

It is well known that proteins are stable only over a limited range of temperatures. Practically all proteins and peptides lose their native structure upon heating above a certain temperature, and several proteins are also known to unfold at low temperatures (cold denaturation).[85] In many cases, the loss of native structure is fully reversible and the protein refolds spontaneously upon a return to physiological temperatures. In a thermodynamic description, the protein ensemble exists in an equilibrium between the folded structure and unfolded conformations, and this equilibrium shifts with temperature. This is demonstrated in Figure 3, which shows changes in the relative contributions of α-helical and random coil conformations of a short peptide, quantified by their respective amide I′ absorption, with temperature. For proteins, the folded−unfolded transition is often cooperative; that is, the equilibrium shifts from completely folded to completely unfolded over a few degrees. Shorter peptides, on the other hand, usually feature a much broader transition region, often ranging over several tens of degrees,[52,86−88] as can be seen in Figure 3.

A sudden increase in temperature (temperature jump) initially leaves the protein ensemble in a conformational distribution that does not correspond to the equilibrium distribution at the new temperature. Observation of the ensuing relaxation towards the new thermal equilibrium allows the

relevant folding dynamics to be determined.[89,90] For cold-denatured proteins, a temperature increase will induce net folding; otherwise the relaxation corresponds to an overall unfolding of the protein. In both cases, if a simple two-state model is assumed (only folded or unfolded proteins present), the equilibrium relaxation time constant τ_{rel} is given by $(k_f + k_u)^{-1}$, where k_f and k_u are the rate constants for folding and unfolding, respectively. Thus, relaxation towards the unfolded protein in fact contains the same information as relaxation towards the folded protein; the separate rate constants can be calculated from τ_{rel} and the equilibrium constant $K = k_f/k_u$. Relaxation dynamics of more complicated systems, which do not exhibit simple two-state equilibrium behaviour, have to be analysed with more sophisticated models,[48] but once again, folding and unfolding relaxation data in principle yield the same information.

The time resolution of temperature jump methods is limited by the time needed to achieve a homogeneous temperature increase. Resistive heaters can produce a significant temperature change within several microseconds;[89] dynamics on the nanosecond and even picosecond timescales are accessible if short laser pulses are used for inducing the temperature jump. For laser-induced temperature jumps in aqueous solution, the laser pulse energy is absorbed either by an inert dye, which undergoes fast internal conversion,[54,91] or directly by the solvent.[92] Direct excitation of weak overtone bands of H_2O near 1.5 μm or D_2O near 2 μm can nowadays be achieved routinely by Raman shifting of Nd:YAG laser pulses[44,48,92] or by difference frequency generation with dye laser pulses.[73] Vibrational relaxation of the excited modes and energy flow from a dye to the solvent occur on picosecond timescales in aqueous solution,[93] and thermal diffusion is fast enough to achieve spatially uniform heating of the solvent in less than 100 ps.[54]

One of the major advantages of temperature jump methods for the investigation of protein-folding processes, distinguishing them from the fast photochemical methods described above, is that protein folding can be observed under native solvent conditions, since there is no need for the addition of denaturants, which are known to affect folding dynamics appreciably.[24,26,31,65] Furthermore, temperature-jump methods rely only on temperature-induced unfolding or folding and are thus applicable to a very broad range of proteins and peptides.

Resistive heating, combined with sensitive tryptophan fluorescence detection and Φ-value analysis,[94] has been used to investigate the folding of cold-denatured barstar on the microsecond to millisecond timescale.[35] An intermediate was found to be formed with a time constant of about 300 μs; this intermediate is characterised by substantial folding of one of the four α-helices of the native structure, but shows only minor burial of the hydrophobic side chains. This fast phase is followed by a slower phase on the 10−100-ms timescale, resulting in the formation of a native-like structure.

The protein most extensively studied by fast laser-induced temperature-jump experiments is apomyoglobin.[95] The native structure of this protein consists of eight α-helices, with helices A, G and H forming a particularly stable compact core.[96] At low temperatures, apomyoglobin undergoes cold denaturation, with only a small amount of residual native structure remaining.[97] Temperature jump initiated folding from this state has been followed by tryptophan fluorescence measurements.[37,41,44] Apomyoglobin has two tryptophan residues, both of which are located on helix A and which, in the native structure, are in close contact with a methionine residue on the loop between helices G and H. Upon formation of the compact AGH core, the methionine quenches the tryptophan fluorescence. AGH core formation times of 4−17 μs were observed upon refolding from the cold-denatured state, with the exact value depending on solvent viscosity, indicating diffusive behaviour. The formation of the AGH core is preceded by a faster phase of fluorescence changes (time constant of 250 ns), which was interpreted as arising from helix formation and/or hydrophobic collapse.

In a complementary series of experiments on apomyoglobin, IR absorbance measurements were used, providing detailed information on secondary structural changes.[55,56,73,98] These experiments did not observe the refolding of cold-denatured apomyoglobin, but studied protein structural relaxations after temperature jumps near the unfolding transition at elevated temperatures. Transitions of "native" helical structures − helices with native-like tertiary contacts − and solvated helices, which are more exposed to the solvent, were monitored separately. For solvated helices, folding relaxation times of around 50 ns were found; these times are similar to those observed for model α-helices (see below). It was concluded that helical segments of real proteins are formed early during folding from the fully denatured state. Helices with native tertiary contacts, on the other hand, displayed much slower relaxation behaviour. This slower phase corresponds to formation/loss of tertiary contacts, and occurs on a timescale (10−100 μs) similar to that of the formation of the AGH core after initiation of folding from the cold-denatured state.

Laser-induced temperature-jump experiments have been performed on a number of other proteins. In one of the first studies in this field, the disruption of β-sheets in ribonuclease A upon a temperature jump above the melting temperature was observed to occur on the nanosecond timescale after an initial induction period of 1 ns.[54] Cytochrome c folding initiated from a partially cold-denatured state yielded a fast quenching of the tryptophan fluorescence in 6 μs, indicating a fast collapse of the protein[44] similar to that observed for reduced cytochrome c folding induced by electron transfer or CO dissociation (see above). Transitions from exponential to nonexponential folding/unfolding dynamics with increasing temperature were found for phosphoglycerate kinase, ubiquitin[38] and the major cold shock protein of *E. coli*,[58] indicating multiple folding pathways on the 10−100 μs timescale. Finally, the structural transition from α_{II}- to α_I-helices in bacteriorhodopsin was found to occur with a time constant of 65 ns.[57]

Temperature-jump experiments have also been used to observe the relaxation dynamics of short de novo peptides.

On the basis of temperature-jump experiments with IR[52,56] and resonance Raman[66] detection, the overall folding of a 21-residue α-helical peptide was reported to occur on the 100-ns timescale. These data were complemented by fluorescence measurements on similar peptides, which were modified with fluorescent labels for detection of the unfolding of the peptide ends.[28,48] The combined results were analysed with kinetic models[48] based on the standard statistical mechanical description of the helix−coil equilibrium.[19,99] It was suggested that the *nucleation* of an α-helix (that is, the formation of the first turn from the random coil structure) occurs on the sub-microsecond timescale, followed by *propagation* of the helix with a single step taking less than 10 ns.[100] Similarly, the folding of a β-hairpin was shown to occur on the timescale of a few microseconds[47] and again the process could be described well by a statistical mechanical model.[101]

A Novel Optical Trigger for Peptide and Protein Folding

As the results summarised in the preceding section show, many steps during the folding of a peptide or protein can occur on the nanosecond or microsecond timescales. A better understanding of protein folding, such as distinction between the different models mentioned above, will only be achieved once these fast steps can be investigated in detail. The direct observation of such fast processes is only possible if they can be initiated on the timescale of interest. In recent years, significant progress has been made in developing new methods for triggering protein folding on short timescales. However, all of the experimental approaches discussed in the previous section have their limitations. Relaxation methods do not allow protein folding to be observed in real-time and no direct structural information can be gained, which complicates any analysis. Rapid-mixing techniques are currently limited to the observation of processes with time constants longer than approx. 30 μs, in spite of the impressive improvement in time resolution that has been achieved in the last years, and it is not obvious that any major reduction of the dead time will be possible soon. The application of photochemical protein-folding triggers, such as ligand dissociation or electron transfer, is restricted to only a few proteins (predominantly heme proteins) and requires the presence of significant amounts of denaturants, which are known to affect protein folding dynamics significantly.[24,26,31,65] Finally, the most general method in use today, initiation of protein structural relaxations by a temperature jump, is limited to the induction of protein unfolding, except for the few proteins that undergo cold denaturation above the freezing point of water.

Thus, it would be highly desirable to develop more generally applicable trigger mechanisms for the initiation of protein folding on short timescales. Such trigger mechanisms should satisfy the following requirements:

(i) *Short timescale:* Any trigger mechanism has to be faster than the processes to be studied. For the case of protein folding, this requires a trigger event that occurs on the nanosecond timescale or faster. Experimental approaches on this timescale are almost exclusively based on photochemical methods.

(ii) *Wide applicability:* It should be possible to use the trigger for a wide range of protein and peptide structures. For this purpose, it should be possible to incorporate any chemical modifications by means of standard procedures such as solid-state peptide synthesis.

(iii) *Physiological conditions:* Preferably, the trigger should operate under native physiological conditions; that is, in aqueous solution at room temperature without excesses of denaturants or other additives.

(iv) *Reversibility:* The phototriggering event should be reversible to allow for multiple excitations, allowing data averaging for good signal-to-noise ratios.

One such general trigger mechanism, which was developed recently, is described in the following section.[59,88] The basic idea is depicted schematically in Scheme 1: A nonnative aryl disulfide cross-linking group provides enough strain to force the peptide or protein into a nonnative, less ordered structure. Laser flash photolysis of the disulfide bond removes this constraint and so initiates folding towards the native structure, which can be monitored by the techniques described above, such as time-resolved IR and CD spectroscopy or, provided that an appropriate chromophore is present, UV/Vis absorbance and fluorescence. Alternatively, the aryl disulfide bond might be used to *stabilise* a peptide or protein under denaturing conditions, in analogy to the stabilising function of cysteine disulfide cross-links found in many proteins. In this case, photolysis of the disulfide bond would initiate the *un*folding reaction. Aryl disulfide bonds are known to cleave in less than 100 ps after excitation by an ultra-short UV laser flash,[102−105] thus providing a fast trigger for protein folding or unfolding.

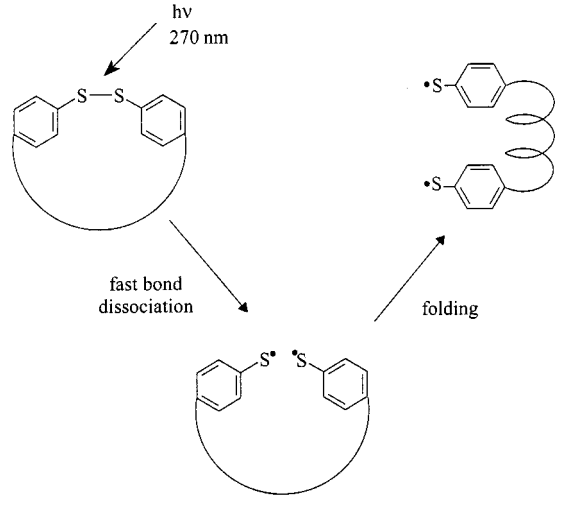

Scheme 1

To demonstrate the general utility of this approach, the helix-coil dynamics of a de novo designed polyalanine peptide, based on the helical peptide reported by Baldwin and

co-workers,[106] was investigated. Aryl disulfide cross-linking groups were incorporated to link the peptide ends, constraining the peptide in a cyclic, less helical conformation. Photocleavage of the disulfide bond on the picosecond timescale removes this constraint, and the peptide begins to fold into its native, more helical structure. This approach allowed the earliest events of helix formation in short peptides to be observed.

Peptide Design

The folding trigger mechanism in Scheme 1 requires the synthesis of an appropriate amino acid containing an arylthiol moiety, which should be suitable for solid-phase peptide synthesis. Synthesis of a polypeptide containing two of these amino acids at locations a significant distance apart in the native structure and oxidation to form a disulfide bond should then yield a peptide constrained in a nonnative conformation.

The synthesis of two cross-linking amino acids, (*S*)-4′-mercaptophenylalanine (thiotyrosine, **1**) and 3-*N*-(4′-mercaptophenyl)-(*S*)-2,3-diaminopropionic acid (aminothiotyrosine, **2**) (Scheme 2) in properly protected forms for use in solid-phase peptide synthesis [Fmoc-**1**(4-MeBzl) and Fmoc-**2**(4-MeBzl)] was described in detail in ref.[88] Protection of the thiol group was found to be provided best by a methylbenzyl (MeBzl) moiety. Thiotyrosine **1** was synthesised in four steps from L-phenylalanine in 30% overall yield, and aminothiotyrosine **2** in six steps, with an overall yield of 40%.

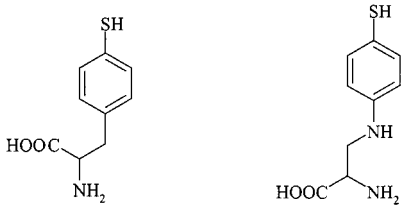

1 (HSY') 2 (HSY")

SY'AAAAKAAAAKAAAAKY'S 3

S S
AAY'AAKAAAAKAAAAY'K 4

SY"AAAAKAAAAKAAAAKY"S 5

A = alanine
K = lysine

Scheme 2

Peptides containing two cross-linking amino acids with protected thiol groups were synthesised on PAL resin, using standard Fmoc chemistry and the stepwise solid-phase method. After peptide synthesis, the thiol-protecting MeBzl groups were removed with anhydrous hydrogen fluoride containing anisole and the peptides were oxidised to the cyclic, disulfide cross-linked peptides with DMSO as oxidant. No protection of the β-amino group of **2** during peptide synthesis was necessary.

Several peptides were synthesised (see Scheme 2). In peptides **3** and **5**, the peptide ends are cross-linked by thiotyrosine **1** and aminothiotyrosine **2**, respectively, whereas in peptide **4** the link was introduced between positions closer together along the peptide. In the latter peptide, the polypeptide ring formed upon cross-linking the thiol groups is even smaller than in the former two, so that the constraint introduced by cyclisation is even more restrictive and results in even less residual helicity (see below).

The helicities of all three cyclic peptides, as well as those of their unconstrained linear analogues (the same peptides before thiol deprotection and oxidation) were assessed by CD and IR spectroscopy.[88] All peptides showed CD spectra typical of α-helical structures, although with quite different amplitudes. The linear peptides all showed significant helicity at low temperatures (70−80% at 1 °C) and a broad melting transition upon heating, in agreement with previous reports for linear polyalanine peptides.[106] Upon cyclisation, however, a significant reduction in the CD signals was observed, corresponding to a reduction of the helicity by a factor of two upon cyclisation of **3** and **5** and by a factor of approx. three for peptide **4**, with the shorter cyclic polypeptide chain. Similar conclusions were obtained from FTIR spectra (see Figure 3). These results confirm that the linear peptides are indeed highly helical and that the helicity is significantly reduced in the cyclic peptides constrained by disulfide bonds. Thus, as anticipated, photolysis of the disulfide bond in peptides **3**−**5** should initiate the relaxation to a more helical conformation, triggering the peptide folding process.

Photochemistry of Aryl Disulfide Cross-Linked Peptides

The idea of using aryl disulfide cross-links as fast triggers for peptide and protein folding arose from reports of very fast splitting of the disulfide bonds in model aryl disulfides after absorption of UV laser flashes.[102−105] To test the concept and to verify that the same process occurs for the aryl disulfide peptide cross-links, transient absorbance measurements with femtosecond time resolution were performed.[59] Peptides **3**−**5** were excited with laser flashes of 140 fs pulse length at 270 nm and the ensuing absorbance changes were measured at different wavelengths in the visible part of the spectrum. For all peptides, the appearance of transient absorbance was observed within the time resolution of the instrument (approx. 200 fs, Figure 4). This transient absorbance was centred at 500 nm for peptides **3** and **4** and at 620 nm for peptide **5** (see inset of Figure 4), which compares well with typical absorbance spectra of *p*-tolylthiyl radicals and *p*-aminophenylthiyl radicals, respectively,[104,107] showing that fast photodissociation of the disulfide bond has indeed taken place.

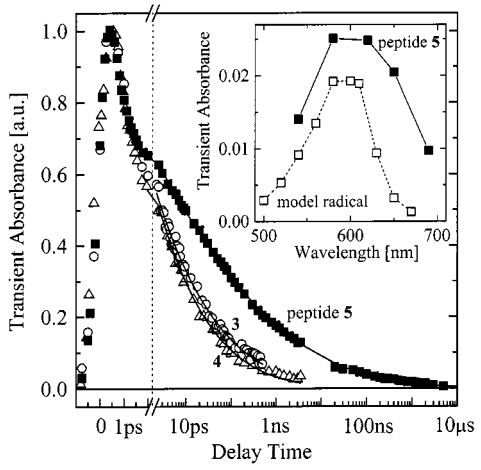

Figure 4. Time dependence of the transient thiyl radical absorbance (normalised to a maximum value of 1) at 500 nm in peptides **3** (open circles) and **4** (open triangles) and at 620 nm in peptide **5** (solid squares) after disulfide bond photolysis with short laser flashes at 270 nm. Note the logarithmic timescale for delay times longer than 2 ps. Solid lines are the best fits of the data after 2 ps to a stretched exponential function $A(t) = A_0 \exp[-(k_0 t)^{\alpha}]$, yielding values for the exponent α of 0.1 ± 0.01 for all peptides. Inset: Transient spectra of aminophenylthiyl radicals at a delay time of 1 ps after photolysis of peptide **5** in water (solid squares) and a model compound, bis(*p*-aminophenyl) disulfide, in ethanol (open squares). Peptide concentration approximately 1 mM in H_2O at 31 °C, time resolution of spectrometer 200 fs. For further experimental details, see ref.[59]

The radicals generated in different peptides show considerable differences in their decay kinetics (Figure 4). For all peptides, a rapid initial decay of the radical absorbance is observed within the first picosecond after generation. For peptides **3** and **4**, which use thiotyrosine **1** as the cross-linker, this rapid decay continues until there are hardly any radicals left after 1 ns. For peptide **5**, with aminothiotyrosine **2** as the cross-linker, on the other hand, the overall recombination of thiyl radicals proceeds much more slowly after 1 ps (note the logarithmic timescale of Figure 4) and radical absorbance can still be detected on the microsecond timescale.

At the low peptide concentrations used in these measurements, the observed fast radical decay has to be attributed to geminate recombination of the radical pairs created at the ends of the peptide; that is, (re-)formation of the original disulfide bond. The different recombination behaviour found for thiotyrosine- and aminothiotyrosine-cross-linked peptides is consistent with work on model compounds. Significant geminate recombination of phenylthiyl radical pairs occurs on the picosecond timescale after photolysis of diphenyl disulfide,[102,104] while no geminate recombination was found for aminophenylthiyl radical pairs created by photolysis of bis(*p*-aminophenyl) disulfide in polar solvents.[104] In fact, these results on aminophenylthiyl radicals stimulated the design of the cross-linking amino acid **2** and peptide **5**, after initial experiments showed fast disulfide bond (re-)formation in peptides **3** and **4**. The inefficient recombination of aminophenylthiyl radicals in polar solvents was attributed to internal charge transfer between the amino group and the sulfur atom on the picosecond timescale.[104] The fact that radical recombination initially proceeds rapidly in all peptides, but slows down after 1 ps for peptide **5**, indicates that such fast internal charge separation also occurs in the aminophenylthiyl groups of the peptide, stabilising the radicals and considerably slowing down disulfide bond (re-)formation.

In summary, fast disulfide bond photolysis was achieved in all peptides **3**–**5**. In **3** and **4**, almost all radical pairs recombine within 1 ns, thus reconstituting the link between the peptide ends and once more fixing the peptides in their original cyclic conformation. This is too fast to permit observation of any significant α-helix formation, as is shown below. In peptide **5**, on the other hand, a significant proportion of the radicals, and thus of unconstrained peptides with open ends, remain even at delay times of 10 ns and longer after photodissociation, which should be enough to permit observation of helix formation dynamics.

Motion of the Peptide Ends

The time dependence of the anisotropy of a transient absorbance signal (that is, the difference between the signals measured with parallel and perpendicular polarisation of pump and probe light[108]) provides information about the rotational motion of a chromophore.[109] Here, the anisotropy of the thiyl radical absorbance for peptide **5** was observed, allowing conclusions to be drawn regarding the motion of the modified tyrosines at the peptide ends. The radical anisotropy decays on the 100-ps timescale (Figure 5). A biexponential fit yielded time constants of 60 ps (relative amplitude 30%) and 600 ps (70%) at 31 °C, and similar results were found at 12 °C.

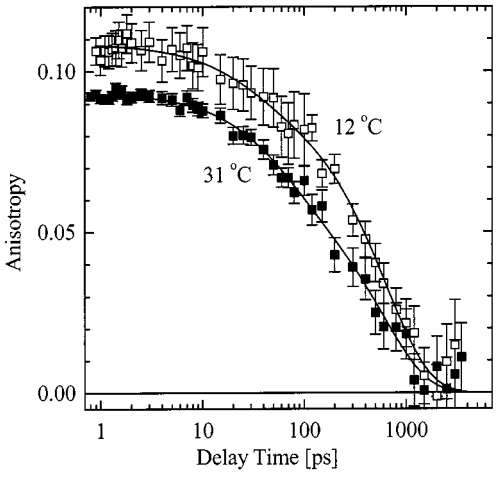

Figure 5. Anisotropy decay of the aminophenylthiyl radical absorbance at 620 nm for peptide **5** at 12 °C (open squares) and 31 °C (solid squares). Solid lines are the best fits of the data to a biexponential decay, as described in the text. Peptide concentration approximately 1 mM in H_2O, time resolution of spectrometer 200 fs. For further experimental details, see ref.[59]

The overall rotational dynamics of a molecule can be theoretically predicted from the Perrin model for rotational diffusion.[110] Rotational diffusion times were estimated for

a representative set of calculated peptide structures,[88] and showed that the shape of the constrained peptides can be approximated by ellipsoids with axis lengths in the range of 9−20 Å. Rotational time constants in water for such ellipsoids are expected to be in the range of 400−650 ps, which compares well with the experimentally observed time constant of 600 ps. This suggests that the slower component of the anisotropy decay originates from the rotational motion of the whole peptide.

The faster component, on the other hand, must be attributed to the motion of a smaller part of the peptide relative to the bulk, most probably a librational motion of the tyrosine ring with respect to the peptide backbone. Analogous biphasic tryptophan fluorescence anisotropy decays have previously been observed for small peptides and proteins, with time constants for the faster decay components ranging from 90 to several hundred ps.[111] In these studies, equilibrium motions were observed and the faster component was assigned to the orientational diffusion of the tryptophan indole ring in its protein pocket. Slightly faster diffusion is expected for the smaller tyrosine, supporting the assignment of the 60 ps anisotropy decay component observed here to orientational diffusion of the tyrosines relative to the whole peptide.

Since it is improbable that large-scale peptide backbone motions can occur without reorientation of the peptide ends, it can be concluded that no significant peptide backbone motions occur on a timescale of less than a few hundred picoseconds. Thus, the process of formation or elongation of the α-helix must proceed on a longer timescale.

α-Helix Formation Dynamics

Time-resolved IR spectroscopy was used for the direct observation of the secondary structural dynamics of peptide **5** after disulfide bond photolysis. Figure 3 shows temperature-dependent equilibrium FTIR spectra of peptide **5**. Two maxima are observed: one at 1672 cm^{-1}, assigned to the trifluoroacetate counterion (TFA), and one which shifts from 1640 cm^{-1} at low temperatures to 1648 cm^{-1} at 62 °C and is assigned to the amide I′ band of the peptide. The difference spectra in Figure 3B confirm that this thermally induced "shift" is in fact due to the transition from a species absorbing at 1633 cm^{-1}, attributable to α-helical segments, to a species absorbing at 1658 cm^{-1}, assigned to the unfolded random coil configuration, in agreement with previous results on short α-helical peptides in D_2O.[52,53] The unconstrained, linear analogue of peptide **5** (that is, the peptide before thiol deprotection and oxidation) has similar IR spectra (data not shown), but with approximately double the helical contribution of the cyclic peptide at the same temperature, in agreement with CD results.[88] After photolysis of the disulfide bond, the partial α-helix of the constrained peptide is expected to grow to the length found in the unconstrained peptide, resulting in a corresponding shift of the amide I′ band, which can be followed by time-resolved IR measurements. Even the fastest steps of this α-helix formation/elongation process on the ps and ns timescales should now be observable, since the bond-breaking takes place on the sub-picosecond timescale.

Such time-resolved IR measurements were performed by photolysis of the disulfide bond of peptide **5** with a laser flash of 140 fs pulse length at 270 nm and probing of the IR absorbance changes with laser pulses of around 6 μm generated by optical parametric amplification. The setup was characterised by a spectral resolution of 15 cm^{-1} and a temporal resolution of better than 1 ps.[59] Figure 6 shows the 2-ns difference spectrum − that is, the spectral changes (with respect to the equilibrium spectrum) observed 2 ns after disulfide bond splitting − of peptide **5** in D_2O at 10 °C. Also shown is the shape of accompanying spectral changes arising from the unavoidable slight heating of D_2O by the photolysis laser pulse. The resulting infrared difference spectrum of peptide **5** itself (solid squares) corresponds to a bleaching or broadening of the amide I′ band at 1640 cm^{-1}.[112] This peptide signal appears within 100 ps after disulfide bond photolysis and decays in parallel with the disappearance of the thiyl radical population (data not shown).

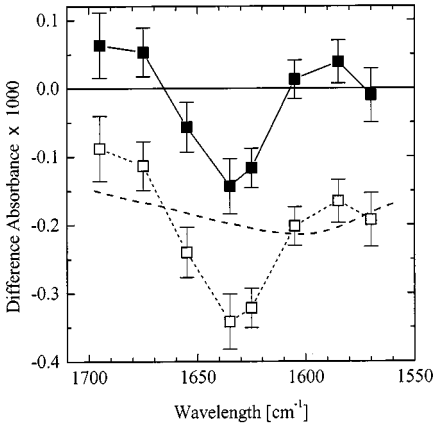

Figure 6. Difference spectrum of peptide **5** in D_2O at 10 °C in the amide I′ region at a delay time of 2 ns after disulfide bond photolysis. Shown are the raw data (open squares), the estimated contribution of D_2O heating (dashed line) and the actual peptide signal (raw data corrected for D_2O heating signal, solid squares). Peptide concentration approximately 10 mM, path length 56 μm, for further experimental details, see text and ref.[59]

The amide I′ band shift expected upon α-helix extension is characterised by a difference spectrum identical to those shown in Figure 3B; that is, a positive band at 1633 cm^{-1} (growth of α-helix) and a negative band at 1658 cm^{-1} (disappearance of random coil). Under the experimental conditions employed, an absorbance increase of approximately 0.15×10^{-3} at 1633 cm^{-1} is expected for the transition to the full α-helix of the unconstrained peptide. In contrast to this expectation, an absorbance *decrease* of that size is observed at 1630 cm^{-1} and the spectral feature does not correspond to that of a shift. Furthermore, the signal appears within 100 ps after disulfide bond photolysis, and thus on a timescale over which significant peptide backbone motions can be ruled out from the radical anisotropy measurements. These results indicate that formation or growth

of the α-helix is not the cause of the observed transient IR signals at 2 ns and that significant helix extension does not occur within 2 ns. In a detailed analysis, it was shown that the observed signal most probably arises from the amide vibrational Stark effect; that is, a shift of the amide I vibrational frequency in the electric field created by the stabilising internal charge separation in the aminothiyl radicals.[59]

It can be concluded that, in peptide **5** at a delay time of 2 ns after disulfide bond splitting, helix propagation towards the extended α-helix of the linear peptide has not yet taken place to any significant extent. Unfortunately, IR measurements at longer delay times were not possible at the time for technical reasons.

Peptide Control of Radical Recombination Dynamics

Photodissociation of the disulfide bond of peptide **5** generates an aminophenylthiyl radical at each peptide end. These radicals recombine geminately on the picosecond to microsecond timescale (Figure 4), thus (re-)forming the original disulfide bond. This behaviour is different to that of analogous aminophenylthiyl radicals generated by photolysis of bis(*p*-aminophenyl) disulfide, which do not undergo geminate recombination, but escape from the solvent cage and undergo nongeminate, diffusion-controlled recombination on the millisecond timescale.[104] Unlike these free radicals, radicals created at the ends of a peptide are tethered together and cannot escape from each other. Also, the radicals' relative motion within the boundaries imposed by the peptide tether is not described by free molecular diffusion, but is controlled by the motion of the peptide backbone to which they are bound. Radical recombination can occur only when the two radicals come into close contact. Thus, radical recombination is governed by the dynamics of peptide end contact formation and a detailed study of the thiyl radical population decay would be expected to yield novel information on internal peptide dynamics.

Radical recombination in peptides **3**, **4** and **5** proceeds with strongly nonexponential kinetics, extending over seven orders of magnitude of time for peptide **5**. The transient radical absorbance, $A(t)$, which is a direct measure of the radical population, can be fitted to a stretched exponential $A(t) = A_0 \exp[-(k_0 t)^{\alpha}]$[113] (see Figure 4). A value of 0.1 ± 0.01 for the exponent α was found for all peptides, implying that the same underlying process is responsible in each case for the kinetics of thiyl radical recombination, despite the significantly faster decay kinetics of peptides **3** and **4**, in comparison with those of peptide **5**.

The transient thiyl radical absorbance, $A(t)$, can also be used to calculate the instantaneous first-order rate constant for geminate radical recombination, $k_{rec}(t) = -[dA(t)/dt]/A(t)$, which describes the probability of recombination at a particular time t. Figure 7 shows the time dependence of this instantaneous rate constant. For delay times above 2 ps, the logarithm of k_{rec} depends linearly on the logarithm of delay time, with a slope of approximately −1 for all three peptides. Thus, the probability of recombination follows a power law in time: $k_{rec}(t) \propto t^{-1}$. This universal power law behaviour with an exponent of −1, observed over seven orders of magnitude of time, and for recombination processes occurring with average radical lifetimes differing by a factor of 1000 (peptides **3** and **4** vs. peptide **5**), is highly unusual.[114] It indicates that the probability of encounters between the radicals (that is, of contact formation between the peptide ends) decreases in inverse proportion to time, even on the microsecond timescale. This is in contrast to the expectation from free three-dimensional diffusion, which predicts that the probability of collisions should decrease as $t^{-1.5}$ until diffusion over the length scale of the peptide has occurred; that is, equilibrium between all possible peptide conformations has been reached, which is expected to occur on the 10−100 ns timescales.[78] At this point the contact formation probability, and thus the recombination rate constant, should assume a constant value. Other explanations for the wide range of t^{-1} behaviour have to be sought. Clearly, this unexpected behaviour can only be understood as a consequence of internal peptide dynamics.

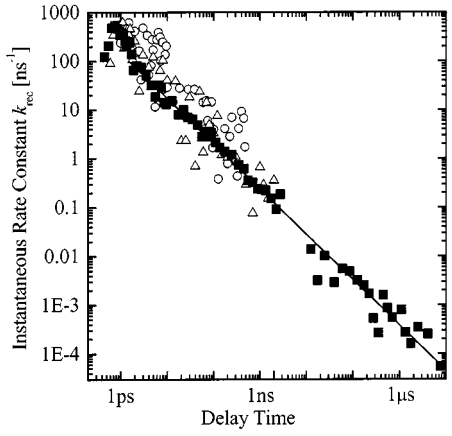

Figure 7. Time dependence of the instantaneous rate constant for radical recombination, $k_{rec}(t) = -[dA(t)/dt]/A(t)$, observed in peptides **3** (open circles), **4** (open triangles) and **5** (solid squares). The solid line is a linear fit of the logarithm of k_{rec} vs. the logarithm of time for peptide **5**, yielding a slope of −0.93 ± 0.02. For peptides **3** and **4**, similar slopes are obtained from the fit, albeit with a larger uncertainty due to the larger noise of the data and the limited range of delay times over which a significant radical population is observed.

Qualitatively, the decrease in the observed peptide end contact formation probability can be understood in terms of a series of conformational changes that, as time progresses, increase the mean peptide end-to-end distance or affect the timescale of peptide motion. After cleavage of the disulfide bond, the thiyl radicals are initially very close, and can recombine rapidly. As time progresses, the fraction of less reactive conformations with longer inter-radical distances increases *and* the peptide becomes less flexible because of α-helix formation. A number of different conformational processes − each operating on different timescales − are known to exist for peptides. Side-chain reorientation associated with changes in the χ_1 and χ_2 angles of the tyrosine residues should be expected to contribute on

the picosecond timescale. It is likely that the faster correlation time associated with the radical absorbance anisotropy decay reflects such side chain reorientations. Diffusion of larger peptide end segments, which are initially in close contact, will set in on the nanosecond timescale.[78] Main-chain conformational changes associated with helix formation, in particular the growth of pre-existing α-helices, occur on the 10 to 100 ns timescale.[48,52] In addition, short peptides are characterised by fluctuating structures, and so a significant part of the peptide ensemble may not have a preinitiated helix at the time of photolysis. Helix formation in these chains only occurs on a longer timescale, probably in the microsecond range,[48] since helix nucleation is significantly slower than helix propagation. Although helix formation may reduce the average end-to-end distance, it will result in less flexible peptide structures and further decrease the probability of contact formation between the peptide ends. Thus, conformational processes occur at time ranges from picoseconds to microseconds, affecting the peptide end contact formation probability and being reflected in the thiyl radical population dynamics. A more quantitative understanding of how these divergent processes contribute to the time dependence of the encounter probability of peptide ends, with the observed uniform t^{-1} power law over at least seven orders of magnitude of time, remains a theoretical challenge.[115]

Conclusions

For a better and more detailed understanding of the principle mechanisms behind peptide and protein folding, it is necessary to investigate the first steps on the route from the unfolded polypeptide to the folded functional protein. To do this, new experimental approaches − in particular, methods to initiate the folding reaction on short timescales which overcome the limitations and shortcomings of previous methods − are required. As discussed here, photodissociation of an aryl disulfide bond constitutes such a fast trigger event. The method is based on the incorporation of cross-linking-modified tyrosines into a peptide or protein at two (or more) positions and oxidation to form an aryl disulfide bond. This cross-link can be photodissociated by a short UV laser flash in less than 1 ps, thus releasing the structural constraint holding the peptide in a nonnative configuration and triggering − on an ultrashort timescale − its relaxation to the native structure. Alternatively, aryl disulfide bonds could be used to stabilise the native structure under denaturing conditions, in analogy to the function of native disulfide bond cross-links, so that the same trigger mechanism could also be used for the initiation of an *un*folding reaction. In both cases, the trigger mechanism operates without any additional requirements, such as the presence of protein cofactors or particular solvent conditions. Even in a larger protein, only a minor distortion of the folded native protein structure adopted after disulfide bond dissociation is to be expected, if the modified tyrosine is replacing an aromatic amino acid. Thus, the novel optical trigger will be useful for the investigation of a wide range of different protein structures.

The initial study, using thiotyrosine **1** to constrain α-helical peptides to less ordered structures, yielded the unforeseen result that the peptide backbone moves so slowly that the radicals are kept in close proximity, enabling efficient recombination of the disulfide bond in less than 1 ns. On the basis of results from model disulfides, aminothiotyrosine **2** was designed as a cross-linking group for which a significant reduction of the inherent recombination was to be expected and indeed was observed. This comprises the first optical trigger that permits the observation of protein or peptide folding dynamics on timescales ranging from picoseconds to microseconds. This trigger satisfies all of the criteria mentioned above for a good trigger mechanism: (i) the trigger event is fast, here faster than 1 ps; (ii) the cross-linker is easily prepared in high yield and can be incorporated into polypeptides by routine solid phase methods;[117] (iii) triggering can be achieved under completely native physiological conditions, although it is not restricted to those conditions and may also be used to examine the effects of nonnative conditions on folding dynamics; and (iv) disulfide bond photolysis is reversible, thus allowing for multiple excitation and extensive data averaging.[118]

In a first application of the new trigger mechanism, aminothiotyrosine **2** was used to link the ends of an α-helical peptide, constraining it in a less helical conformation. A UV laser flash was used to trigger the transition to the native, more helical conformation. Time-resolved absorbance measurements showed that no major peptide backbone motions take place before 500 ps and that the overall α-helix elongation process in short peptides takes longer than a few nanoseconds. This is consistent with recent results obtained more indirectly from the *un*folding dynamics of short helical peptides after a temperature jump.[48,52] Recombination of thiyl radicals at the peptide ends proceeds with an unusual power law dependence of the recombination rate constant over seven orders of magnitude of time, which is clearly governed by the internal peptide dynamics.

Outlook

Photodissociation of aryl disulfide cross-links based on aminothiotyrosine **2** provides a method well suited for initiating peptide and protein (un)folding on short timescales and thus for the investigation of the first, ultrafast steps of this process. One feature of this trigger mechanism that could be further optimised is the rate of thiyl radical recombination, which results in the (re-)formation of the cross-link and occurs mainly on the nanosecond timescale, thus hindering the observation of processes that are significantly slower.[119] Slower recombination could be achieved by the use of triplet-sensitised photodissociation, which has been observed for model aryl disulfides.[120] Fast triplet-sensitised bond dissociation may be possible by attachment of

a triplet sensitiser chromophore directly to (amino)thiotyrosine[121] or to the peptide in the immediate vicinity of the disulfide bond. Excitation of the sensitiser, followed by fast intrasystem crossing and triplet energy transfer to the disulfide moiety, would then result in a *triplet*-phased thiyl radical pair. The recombination of this radical pair to the *singlet* ground state would be hindered by the need to overcome the spin barrier. Although triplet sensitisation may result in somewhat slower photodissociation than that achievable by direct excitation of the aryl disulfide, it can be designed to occur on the sub-nanosecond timescale,[121] which makes it fast enough for the investigation of secondary structure formation on the 10 ns to 10 μs timescale. For the successful implementation of triplet-sensitised photodissociation, it will be necessary to modify aminothiotyrosine **2** further, or to develop a synthetic amino acid containing a triplet-sensitising group, which could then be positioned in the immediate vicinity of the disulfide bond.

Although photolysis of aryl disulfide cross-links as a fast trigger for peptide and protein folding gives access to a wide range of applications, particularly if thiyl radical recombination could be slowed down, there are also other synthetic approaches that may provide fast trigger function. One mechanism, based on the incorporation of an intramolecular azobenzene cross-linker, has been suggested recently. Photoisomerisation of azobenzene was shown to result in significant changes in the helicity of specifically designed short α-helical peptides,[122] but can also be used to induce transitions between turn and less ordered or extended conformations.[123,124] Azobenzene photoisomerisation, which is very fast and fully reversible,[125] in principle provides a trigger mechanism fulfilling the above criteria. One drawback of this approach is the fact that the azobenzene cross-linker remains fully intact, resulting in a nonnative constraint even after the trigger event. Therefore, the ensuing folding process is not that of a constraint-free peptide, as in the approach discussed above. No time-resolved investigations on azobenzene cross-linked peptides have yet been reported. In a similar approach, which uses a photoisomerisable side chain in a linear peptide rather than cross-linked peptides, the isomerisation of *p*-phenylazo-L-phenylalanine has been shown to result in a transition from β-sheet to α-helix structure,[126] showing potential for use as a fast trigger of conformational changes.

The application of a novel trigger mechanism will often be particularly simple for short peptides. It is possible to design synthetic amino acids so that they can easily be incorporated into a peptide during stepwise solid-phase peptide synthesis. Folding studies on short peptides avoid the heterogeneous mixture of structural elements found in larger proteins and are ideally suited for the acquisition of clear information relating to the intrinsic dynamics of particular secondary structural motifs. Synthetic peptides offer the further advantage of an easily altered primary sequence, which will allow the detailed investigation of internal factors governing folding dynamics and mechanism, such as side chain−side chain or side chain−backbone interactions. Such detailed results are necessary for the unambiguous interpretation of the observed folding dynamics of naturally occurring proteins, which, because of their complexity, will remain difficult to analyse without more detailed knowledge of the folding dynamics of their components.

The few ground-breaking studies investigating fast folding dynamics of short peptides performed so far have all made use of the temperature-jump method,[47,48,52] in which a temperature jump induces a shift of the peptide structural equilibrium from folded to more unfolded conformations. For certain applications, it would be advantageous to combine such results on *un*folding dynamics with results on *folding* dynamics, obtained with new optical triggers. Although both sets of results in principle contain the same information on details of the folding/unfolding dynamics, in practice the two methods often yield complementary information, as some aspects of the dynamics are more easily observed during the folding reaction, whereas others are more pronounced in the unfolding reaction. Under most experimental conditions, for example, the dynamics associated with α-helix nucleation do not strongly contribute to the relaxation of an α-helical peptide after a temperature jump, whereas they are expected to dominate the folding from the completely unfolded peptide.[100] Thus, the parallel use of both methods for the same peptide would allow for more comprehensive analysis of the folding process. This could be achieved, for example, by the parallel investigation of the folding dynamics of peptide **5** after disulfide bond photolysis and the unfolding dynamics of the linear analogue of peptide **5** (containing the modified tyrosines in their protected form) after a temperature jump.

In conclusion, it is to be expected that application of the aryl disulfide bond photodissociation trigger, and similar trigger mechanisms, based on photochemical processes in modified amino acids still to be developed, will considerably enhance our understanding of fast protein-folding dynamics. Such trigger mechanisms would initially be used for direct observation of the formation dynamics of specific secondary structural elements in small de novo peptides. In the long term, however, they should also find application for the investigation of larger proteins. As yet, the search for useful new trigger mechanisms is only at its beginning. The challenge of finding such trigger mechanisms can only be tackled by intensive interdisciplinary collaboration between organic chemists, biophysicists and biologists. In this collaboration, the organic chemists will provide suitable modifications of amino acids and thus of peptides or proteins, which the biophysicists will investigate with their fast (usually laser-based) methods, giving feedback for further improvement, while the biologists, who posed the original protein folding problem, will provide the wider context for interpreting the results.

Acknowledgments

I would like to thank Prof. Robin Hochstrasser, University of Pennsylvania, for the interesting and most stimulating time in his laboratory, during which we investigated the novel optical trigger for protein folding described in this article. I am also most grateful

to Prof. Bill DeGrado and Dr. Helen Lu at the University of Pennsylvania, who developed this trigger, and to Ed Gooding and Yuriy Kholodenko for assistance with the time-resolved measurements. I would also like to thank the referees for most helpful comments and suggestions for improving the manuscript.

[1] C. B. Anfinsen, *Science* **1973**, *181*, 223−230.
[2] [2a] A. Liwo, J. Lee, D. R. Ripoll, J. Pillardy, H. A. Scheraga, *Proc. Natl. Acad. Sci. USA* **1999**, *96*, 5482−5485. − [2b] M. Vasquez, G. Nemethy, H. A. Scheraga, *Chem. Rev.* **1994**, *94*, 2183−2239.
[3] [3a] W. F. DeGrado, *Science* **1997**, *278*, 80−81. − [3b] B. I. Dahiyat, S. L. Mayo, *Science* **1997**, *278*, 82−87. − [3c] S. E. Radford, C. M. Dobson, *Cell* **1999**, *97*, 291−298. − [3d] T. Kortemme, M. Ramírez-Alvarado, L. Serrano, *Science* **1998**, *281*, 253−256. − [3e] P. B. Harbury, J. J. Plecs, B. Tidor, T. Alber, P. S. Kim, *Science* **1998**, *282*, 1462−1467.
[4] C. Levinthal, *J. Chim. Phys. Phys.-Chim. Biol.* **1968**, *65*, 44−45.
[5] [5a] O. B. Ptitsyn, *J. Protein Chem.* **1987**, *6*, 273−293. − [5b] O. B. Ptitsyn, *Protein Eng.* **1994**, *7*, 593−596. − [5c] M. Karplus, D. L. Weaver, *Nature* **1976**, *260*, 404−406. − [5d] M. Karplus, D. L. Weaver, *Prot. Sci.* **1994**, *3*, 650−668.
[6] P. S. Kim, R. L. Baldwin, *Annu. Rev. Biochem.* **1982**, *51*, 459−489.
[7] P. S. Kim, R. L. Baldwin, *Annu. Rev. Biochem.* **1990**, *59*, 631−660.
[8] K. A. Dill, *Biochemistry* **1985**, *24*, 1501−1509.
[9] K. A. Dill, S. Bromberg, K. Yue, K. M. Fiebig, D. P. Yee, P. D. Thomas, H. S. Chan, *Protein Sci.* **1995**, *4*, 561−602.
[10] [10a] T. R. Sosnick, L. Mayne, S. W. Englander, *Proteins* **1996**, *24*, 413−426. − [10b] T. R. Sosnick, S. Jackson, R. R. Wilk, S. W. Englander, W. F. DeGrado, *Proteins* **1996**, *24*, 427−432.
[11] [11a] D. E. Otzen, L. S. Itzhaki, N. F. ElMasry, S. E. Jackson, A. R. Fersht, *Proc. Natl. Acad. Sci. USA* **1994**, *91*, 10422−10425. − [11b] V. I. Abkevich, A. M. Gutin, E. I. Shakhnovich, *Biochemistry* **1994**, *33*, 10026−10036. − [11c] Z. Guo, D. Thirumalai, *Biopolymers* **1995**, *36*, 83−102.
[12] A. R. Fersht, *Curr. Opin. Struct. Biol.* **1997**, *7*, 3−9.
[13] [13a] T. E. Creighton, D. P., *J. Mol. Biol.* **1984**, *179*, 497−526. − [13b] J. S. Weissman, P. S. Kim, *Science* **1991**, *253*, 1386−1393.
[14] J. S. Weissman, P. S. Kim, *Cell* **1992**, *71*, 841−851.
[15] X. Zhu, Y. Ohta, F. Jordan, M. Inouye, *Nature* **1989**, *339*, 483−484.
[16] [16a] K.-M. Pan, M. Baldwin, J. Nguyen, M. Gasset, A. Serban, D. Groth, I. Mehlhorn, Z. Huang, R. J. Fletterick, F. E. Cohen, S. B. Prusiner, *Proc. Natl. Acad. Sci. USA* **1993**, *90*, 10962−10966. − [16b] P. M. Harrison, P. Bamborough, V. Daggett, S. B. Prusiner, F. E. Cohen, *Curr. Opin. Struct. Biol.* **1997**, *7*, 53−59. − [16c] S. B. Prusiner, *Proc. Natl. Acad. Sci. USA* **1998**, *95*, 13363−13383. − [16d] H. Mihara, Y. Takahashi, *Curr. Opin. Struct. Biol.* **1997**, *7*, 501−508.
[17] [17a] R. L. Baldwin, G. D. Rose, *Trends Biochem. Sci.* **1999**, *24*, 26−33. − [17b] R. L. Baldwin, G. D. Rose, *Trends Biochem. Sci.* **1999**, *24*, 77−83. − [17c] S.-R. Yeh, D. L. Rousseau, *Nat. Struct. Biol.* **2000**, *7*, 443−445.
[18] [18a] O. B. Ptitsyn, *Adv. Protein Chem.* **1995**, *47*, 83−229. − [18b] M. Bycroft, A. Matouschek, J. T. Kellis Jr., L. Serrano, A. R. Fersht, *Nature* **1990**, *346*, 488−490. − [18c] W. A. Houry, D. M. Rothwarf, H. A. Scheraga, *Nat. Struct. Biol.* **1995**, *2*, 495−503. − [18d] G. A. Elöve, A. F. Chaffotte, H. Roder, M. E. Goldberg, *Biochemistry* **1992**, *31*, 6876−6883. − [18e] P. A. Jennings, P. E. Wright, *Science* **1993**, *262*, 892−895. − [18f] S. E. Radford, C. M. Dobson, P. A. Evans, *Nature* **1992**, *358*, 302−307.
[19] B. H. Zimm, J. K. Bragg, *J. Chem. Phys.* **1959**, *31*, 526−535.
[20] C. L. Brooks, *J. Phys. Chem.* **1996**, *100*, 2546−2549.
[21] [21a] J. Tirado-Rives, W. L. Jorgensen, *Biochemistry* **1991**, *30*, 3864−3871. − [21b] K. V. Soman, A. Karimi, D. A. Case, *Biopolymers* **1993**, *33*, 1567−1580. − [21c] T. Lazaridis, M. Karplus, *Science* **1997**, *278*, 1928−1931. − [21d] Y. Duan, L. Wang, P. A. Kollman, *Proc. Natl. Acad. Sci. USA* **1998**, *95*, 9897−9902. − [21e] Y. Duan, A. Kollman, *Science* **1998**, *282*, 740−744.
[22] M. C. R. Shastry, S. D. Luck, H. Roder, *Biophys. J.* **1998**, *74*, 2714−2721.
[23] S. Takahashi, S.-R. Yeh, T. K. Das, C.-K. Chan, D. S. Gottfried, D. L. Rousseau, *Nat. Struct. Biol.* **1997**, *4*, 44−50.
[24] C.-K. Chan, Y. Hu, S. Takahashi, D. L. Rousseau, W. A. Eaton, J. Hofrichter, *Proc. Natl. Acad. Sci. USA* **1997**, *94*, 1779−1784.
[25] C. M. Jones, E. R. Henry, Y. Hu, C. K. Chan, S. D. Luck, A. Bhuyan, H. Roder, J. Hofrichter, W. A. Eaton, *Proc. Natl. Acad. Sci. USA* **1993**, *90*, 11860−11864.
[26] T. Pascher, J. P. Chesick, J. R. Winkler, H. B. Gray, *Science* **1996**, *271*, 1558−1560.
[27] P. Wittung-Stafshede, H. B. Gray, J. R. Winkler, *J. Am. Chem. Soc.* **1997**, *119*, 9562−9563.
[28] W. A. Eaton, V. Muñoz, P. A. Thompson, E. R. Henry, J. Hofrichter, *Acc. Chem. Res.* **1998**, *31*, 745−753.
[29] J. R. Telford, P. Wittung-Stafshede, H. B. Gray, J. R. Winkler, *Acc. Chem. Res.* **1998**, *31*, 755−763.
[30] E. Chen, M. J. Wood, A. L. Fink, D. S. Kliger, *Biochemistry* **1998**, *37*, 5589−5598.
[31] P. Wittung-Stafshede, J. C. Lee, J. R. Winkler, H. B. Gray, *Proc. Natl. Acad. Sci. USA* **1999**, *96*, 6587−6590.
[32] J. R. Telford, F. A. Tezcan, H. B. Gray, J. R. Winkler, *Biochemistry* **1999**, *38*, 1944−1949.
[33] S. J. Hagen, J. Hofrichter, A. Szabo, W. A. Eation, *Proc. Natl. Acad. Sci. USA* **1996**, *93*, 11615−11617.
[34] M. R. Eftink, *Biophys. J.* **1994**, *66*, 482−501.
[35] [35a] B. Nölting, R. Golbik, A. R. Fersht, *Proc. Natl. Acad. Sci. USA* **1995**, *92*, 10668−10672. − [35b] B. Nölting, R. Golbik, J. L. Neira, A. S. Soler-Gonzalez, G. Schreiber, A. R. Fersht, *Proc. Natl. Acad. Sci. USA* **1997**, *94*, 826−830.
[36] M. Jamin, S.-R. Yeh, D. L. Rousseau, R. L. Baldwin, *J. Mol. Biol.* **1999**, *292*, 731−740.
[37] R. M. Ballew, J. Sabelko, M. Gruebele, *Nat. Struct. Biol.* **1996**, *3*, 923−926.
[38] J. Sabelko, J. Ervin, M. Gruebele, *Proc. Natl. Acad. Sci. USA* **1999**, *96*, 6031−6036.
[39] M. P. Lillo, J. M. Beechem, *Biochemistry* **1997**, *36*, 11261−11272.
[40] C.-K. Chan, J. Hofrichter, W. A. Eaton, *Science* **1996**, *274*, 628−629.
[41] R. M. Ballew, J. Sabelko, M. Gruebele, *Proc. Natl. Acad. Sci. USA* **1996**, *93*, 5759−5764.
[42] M. C. R. Shastry, H. Roder, *Nat. Struct. Biol.* **1998**, *5*, 385−392.
[43] M. C. R. Shastry, J. M. Sauder, H. Roder, *Acc. Chem. Res.* **1998**, *31*, 717−725.
[44] M. Gruebele, J. Sabelko, R. Ballew, J. Ervin, *Acc. Chem. Res.* **1998**, *31*, 699−707.
[45] S.-R. Yeh, D. L. Rousseau, *J. Biol. Chem.* **1999**, *274*, 17853−17859.
[46] J. G. Lyubovitsky, J. R. Telford, J. R. Winkler, H. B. Gray, *J. Inorg. Biochem.* **1999**, *74*, 216−216.
[47] V. Muñoz, P. A. Thompson, J. Hofrichter, W. A. Eaton, *Nature* **1997**, *390*, 196−199.
[48] [48a] P. A. Thompson, W. A. Eaton, J. Hofrichter, *Biochemistry* **1997**, *36*, 9200−9210. − [48b] P. A. Thompson, V. Muñoz, G. S. Jas, E. R. Henry, W. A. Eaton, J. Hofrichter, *J. Phys. Chem. B* **2000**, *104*, 378−389.
[49] [49a] T. Miyazawa, E. R. Blout, *J. Am. Chem. Soc.* **1961**, *83*, 712−719. − [49b] T. Miyazawa in *Poly-α-amino acids − Protein models for conformational studies* (Ed.: G. D. Fasman), Arnold, London, **1967**, pp. 69−103. − [49c] S. Krimm, J. Bandekar, *Adv. Protein Chem.* **1986**, *38*, 181−364. − [49d] H. Susi, D. M. Byler, *Methods Enzymol.* **1986**, *130*, 290−311. − [49e] W. K. Surewicz, H. H. Mantsch, *Biochim. Biophys. Acta* **1988**, *952*, 115−130. − [49f] W. K. Surewicz, H. H. Mantsch, D. Chapman, *Biochem-*

istry **1993**, *32*, 389−394. − [49g] J. L. R. Arrondo, A. Muga, J. Castresana, F. M. Goñi, *Prog. Biophys. Molec. Biol.* **1993**, *59*, 23−56.
[50] T. Miyazawa, *J. Chem. Phys.* **1960**, *32*, 1647−1652.
[51] The prime indicates deuterated amides, which are observed when D_2O is used instead of H_2O as solvent to avoid the strong H_2O absorption in the amide I region.
[52] S. Williams, T. P. Causgrove, R. Gilmanshin, K. S. Fang, R. H. Callender, W. H. Woodruff, R. B. Dyer, *Biochemistry* **1996**, *35*, 691−697.
[53] S. M. Decatur, J. Antonic, *J. Am. Chem. Soc.* **1999**, *121*, 11914−11915.
[54] C. M. Phillips, Y. Mizutani, R. M. Hochstrasser, *Proc. Natl. Acad. Sci. USA* **1995**, *92*, 7292−7296.
[55] [55a] R. Gilmanshin, S. Williams, R. H. Callender, W. H. Woodruff, R. B. Dyer, *Proc. Natl. Acad. Sci. USA* **1997**, *94*, 3709−3713. − [55b] R. Gilmanshin, S. Williams, R. H. Callender, W. H. Woodruff, R. B. Dyer, *Biochemistry* **1997**, *36*, 15006−15012.
[56] R. B. Dyer, F. Gai, W. H. Woodruff, R. Gilmanshin, R. H. Callender, *Acc. Chem. Res.* **1998**, *31*, 709−716.
[57] J. Wang, M. A. El-Sayed, *Biophys. J.* **1999**, *76*, 2777−2783.
[58] D. T. Leeson, F. Gai, H. M. Rodriguez, L. M. Gregoret, R. B. Dyer, *Proc. Natl. Acad. Sci. USA* **2000**, *97*, 2527−2532.
[59] M. Volk, Y. Kholodenko, H. S. M. Lu, E. A. Gooding, W. F. DeGrado, R. M. Hochstrasser, *J. Phys. Chem. B* **1997**, *101*, 8607−8616.
[60] T. Elsaesser, J. G. Fujimoto, D. A. Wiersma, W. Zinth (Eds.), *Ultrafast Phenomena XI*, Springer-Verlag, Berlin, **1998**.
[61] *Circular Dichroism, the Conformational Analysis of Biomolecules* (Ed.: G. Fasman), Plenum Publishers, New York, **1996**.
[62] E. Chen, P. Wittung-Stafshede, D. S. Kliger, *J. Am. Chem. Soc.* **1999**, *121*, 3811−3817.
[63] Z. Chi, X. G. Chen, J. S. W. Holtz, S. A. Asher, *Biochemistry* **1998**, *37*, 2854−2864.
[64] [64a] S.-R. Yeh, S. Takahashi, B. Fan, D. L. Rousseau, *Nat. Struct. Biol.* **1997**, *4*, 51−56. − [64b] S.-R. Yeh, S. Han, D. L. Rousseau, *Acc. Chem. Res.* **1998**, *31*, 727−736.
[65] S.-R. Yeh, D. L. Rousseau, *Nat. Struct. Biol.* **1998**, *5*, 222−228.
[66] I. K. Lednev, A. S. Karnoup, M. C. Sparrow, S. A. Asher, *J. Am. Chem. Soc.* **1999**, *121*, 4076−4077.
[67] E. Chen, R. A. Goldbeck, D. S. Kliger, *Annu. Rev. Biophys. Biomol. Struct.* **1997**, *26*, 327−355.
[68] R. A. Goldbeck, Y. G. Thomas, E. Chen, R. M. Esquerra, D. S. Kliger, *Proc. Natl. Acad. Sci. USA* **1999**, *96*, 2782−2787.
[69] V. M. Grigoryants, A. V. Veselov, C. P. Scholes, *Biophys. J.* **2000**, *78*, 2702−2708.
[70] L. Pollack, M. W. Tate, N. C. Darnton, J. B. Knight, S. M. Gruner, W. A. Eaton, R. H. Austin, *Proc. Natl. Acad. Sci. USA* **1999**, *96*, 10115−10117.
[71] S. Abbruzzetti, E. Crema, L. Masino, A. Vecli, C. Viappiani, J. R. Small, L. J. Libertini, E. W. Small, *Biophys. J.* **2000**, *78*, 405−415.
[72] W. A. Eaton, P. A. Thompson, C. K. Chan, S. J. Hagen, J. Hofrichter, *Structure* **1996**, *4*, 1133−1139.
[73] R. H. Callender, R. B. Dyer, R. Gilmanshin, W. H. Woodruff, *Annu. Rev. Phys. Chem.* **1998**, *49*, 173−202.
[74] M. Gruebele, *Annu. Rev. Phys. Chem.* **1999**, *50*, 485−516.
[75] D. J. Brockwell, D. A. Smith, S. E. Radford, *Curr. Opin. Struct. Biol.* **2000**, *10*, 16−25.
[76] [76a] G. Schwarz, J. Seelig, *Biopolymers* **1968**, *6*, 1263−1277. − [76b] G. G. Hammes, P. B. Roberts, *J. Am. Chem. Soc.* **1969**, *91*, 1812−1816. − [76c] B. Gruenewald, C. U. Nicola, A. Lustig, G. Schwarz, H. Klump, *Biophys. Chem.* **1979**, *9*, 137−147.
[77] B. Nölting, M. Jiang, S. G. Sligar, *J. Am. Chem. Soc.* **1993**, *115*, 9879−9882.
[78] [78a] O. Bieri, J. Wirz, B. Hellrung, M. Schutkowski, M. Drewello, T. Kiefhaber, *Proc. Natl. Acad. Sci. USA* **1999**, *96*, 9597−9601. − [78b] L. J. Lapidus, W. A. Eaton, J. Hofrichter, *Proc. Natl. Acad. Sci. USA* **2000**, *97*, 7220−7225.
[79] S. Akiyama, S. Takahashi, K. Ishimori, I. Morishima, *Nat. Struct. Biol.* **2000**, *7*, 514−520.
[80] S. J. Hagen, J. Hofrichter, W. A. Eaton, *J. Phys. Chem. B* **1997**, *101*, 2352−2365.
[81] P. Wittung-Stafshede, B. G. Malmström, J. R. Winkler, H. B. Gray, *J. Phys. Chem. A* **1998**, *102*, 5599−5601.
[82] J. H. Clark, S. L. Shapiro, A. J. Campillo, K. R. Winn, *J. Am. Chem. Soc.* **1979**, *101*, 746−748.
[83] E. Pines, D. Huppert, M. Gutman, N. Nachliel, M. Fishman, *J. Phys. Chem.* **1986**, *90*, 6366−6370.
[84] M. Gutman, *Methods Enzymol.* **1986**, *127*, 522−538.
[85] [85a] P. L. Privalov, *Annu. Rev. Biophys. Biophys. Chem.* **1989**, *18*, 47−69. − [85b] P. L. Privalov, *CRC Crit. Rev. Biochem.* **1990**, *25*, 281−305.
[86] B. H. Zimm, P. Doty, K. Iso, *Proc. Natl. Acad. Sci. USA* **1959**, *45*, 1601−1607.
[87] S. Marqusee, R. L. Baldwin, *Proc. Natl. Acad. Sci. USA* **1987**, *84*, 8898−8902.
[88] H. S. M. Lu, M. Volk, Y. Kholodenko, E. Gooding, R. M. H. Hochstrasser, W. F. DeGrado, *J. Am. Chem. Soc.* **1997**, *119*, 7173−7180.
[89] G. Czerlinski, M. Eigen, *Z. Elektrochem.* **1959**, *63*, 652−661.
[90] M. Eigen, L. DeMaeyer, in *Technique of Organic Chemistry*, vol. VIII, 2 (Eds.: S. L. Friess, E. S. Lewis, A. Weissberger), Interscience, New York, **1963**, pp. 895−1054.
[91] H. Staerk, G. Czerlinski, *Nature* **1965**, *205*, 63−64.
[92] D. H. Turner, G. W. Flynn, N. Sutin, J. V. Beitz, *J. Am. Chem. Soc.* **1972**, *94*, 1554−1559.
[93] T. Lian, B. Locke, Y. Kholodenko, R. M. Hochstrasser, *J. Phys. Chem.* **1994**, *98*, 11648−11656.
[94] In Φ-value analysis, the effect of single-site mutations on the free energy of the transition state of a folding reaction is quantified by comparing the effect of the mutation on the folding kinetics with its effect on the equilibrium free energy difference between folded and unfolded state. The Φ-value thus determined allows conclusions on structural changes occurring in the transition state: A. R. Fersht, A. Matouschek, L. Serrano, *J. Mol. Biol.* **1992**, *224*, 771−782.
[95] Apomyoglobin denotes myoglobin without the heme cofactor.
[96] S. V. Evans, G. D. Brayer, *J. Biol. Chem.* **1988**, *263*, 4263−4268.
[97] J. Sabelko, J. Ervin, M. Gruebele, *J. Phys. Chem. B* **1998**, *102*, 1806−1819.
[98] R. Gilmanshin, R. H. Callender, R. B. Dyer, *Nat. Struct. Biol.* **1998**, *5*, 363−365.
[99] S. Lifson, A. Roig, *J. Chem. Phys.* **1961**, *34*, 1963−1974.
[100] Results for α-helix folding after fast dilution of denaturants indicating helix nucleation on the *milli*second timescale have recently been reported, thus raising doubts about the conclusion of sub-*micro*second nucleation from temperature-jump experiments: D. T. Clarke, A. J. Doig, B. J. Stapley, G. R. Jones, *Proc. Natl. Acad. Sci. USA* **1999**, *96*, 7232−7237.
[101] V. Muñoz, E. R. Henry, J. Hofrichter, W. A. Eaton, *Proc. Natl. Acad. Sci. USA* **1998**, *95*, 5872−5879.
[102] T. W. Scott, S. N. Liu, *J. Phys. Chem.* **1989**, *93*, 1393−1396.
[103] N. P. Ernsting, *Chem. Phys. Lett.* **1990**, *166*, 221−226.
[104] N. A. Borisevich, N. A. Lysak, S. V. Melnichuk, S. A. Tikhomirov, G. B. Tolstorozhev, in *Ultrafast Phenomena in Spectroscopy*, vol. 49 (Eds.: E. Klose, B. Wilhelmi), Springer-Verlag, Berlin, Heidelberg, **1990**, pp. 276−281.
[105] Y. Hirata, Y. Niga, T. Okada, *Chem. Phys. Lett.* **1994**, *221*, 283−288.
[106] S. Marqusee, V. H. Robbins, R. L. Baldwin, *Proc. Natl. Acad. Sci. USA* **1989**, *86*, 5286−5290.
[107] [107a] F. C. Thyrion, *J. Phys. Chem.* **1973**, *77*, 1478−1482. − [107b] G. H. Morine, R. R. Kuntz, *Chem. Phys. Lett.* **1979**, *67*, 552−554. − [107c] R. R. Lembke, L. V. Natarajan, R. R. Kuntz, *J. Photochem.* **1983**, *21*, 814−823.
[108] The anisotropy $r(t)$ at time t is defined as

$$r(t) = \frac{A_{\parallel}(t) - A_{\perp}(t)}{A_{\parallel}(t) + 2A_{\perp}(t)}$$

where $A_{\parallel}(t)$ and $A_{\perp}(t)$ denote the transient absorbance at time t measured with parallel and perpendicular polarisation of pump and probe light, respectively.

[109] [109a] T. J. Chuang, K. B. Eisenthal, *J. Chem. Phys.* **1972**, *57*, 5094−5097. – [109b] G. G. Belford, R. L. Belford, G. Weber, *Proc. Natl. Acad. Sci. USA* **1972**, *69*, 1392−1393.

[110] F. Perrin, *J. Phys. Radium* **1934**, *5*, 497.

[111] [111a] I. Munro, I. Pecht, L. Stryer, *Proc. Natl. Acad. Sci. USA* **1979**, *76*, 56−60. – [111b] J. B. A. Ross, K. W. Rousslang, L. Brand, *Biochemistry* **1981**, *20*, 4361−4369. – [111c] C. D. Tran, G. S. Beddard, A. D. Osborne, *Biochim. Biophys. Acta* **1982**, *709*, 256−264.

[112] Definite distinction between bleaching and broadening of the amide I′ band was not possible, since the size of the induced temperature increase (of less than 0.5 °C) and thus the amplitude of the D_2O signal are not known with sufficient accuracy.

[113] A. Plonka in *Time Dependent Reactivity of Species in Condensed Media* (Eds.: G. Berthier, M. J. S. Dewar, H. Fischer, K. Fukui, G. G. Hall, H. Hartmann, H. H. Jaffe, J. Jortner, W. Kutzelnigg, K. Ruedenberg, J. Tomasi), Springer-Verlag, Berlin, **1988**, p. 151.

[114] If radical recombination followed a diffusion-controlled, bimolecular second-order rate law, involving the recombination of radicals from different peptides, such a power law of t^{-1} for the apparent first-order instantaneous rate constant would be observed at sufficiently long times. However, a simple estimate shows that such a process would be much too slow to contribute significantly to the observed recombination, given the low concentration of radicals (approximately 10^{-5} M) and assuming a reasonable bimolecular rate constant of 10^9 $M^{-1}s^{-1}$.

[115] R. Metzler, J. Klafter, J. Jortner, M. Volk, *Chem. Phys. Lett.* **1998**, *293*, 477−484.

[116] Intrapeptide contact formation has recently been investigated by triplet energy transfer (ref.[78]). In these experiments, the triplet state of a chromophore at one peptide end is quenched upon contact formation with a chromophore attached to the opposite end of a flexible peptide. This probe of contact formation dynamics is strongly analogous to the radical recombination upon contact formation investigated here. In contrast to the observed extremely nonexponential radical recombination, however, exponential triplet decays (on the nanosecond timescale) were found in all cases. These different results can be explained by the different initial peptide conformations encountered in the two sets of experiments. In the triplet transfer experiments, the variety of peptide conformations at the moment of excitation corresponds to the equilibrium distribution, and contact formation is achieved by equilibrium fluctuations with a time-independent probability. In the radical recombination experiments, on the other hand, immediately after disulfide bond photolysis, all peptides are in conformations with small end-to-end distances: i.e., the distribution is far from equilibrium. Relaxation towards equilibrium results in a fast increase of the mean end-to-end distance and so the probability of contact formation decreases with time, as discussed in the text. For the triplet transfer experiments, moreover, peptides without internal structure were used, avoiding any internal peptide process apart from polypeptide chain diffusion. For the peptides used in the disulfide photolysis study, in contrast, additional processes such as α-helix nucleation and growth are expected to contribute to the internal peptide dynamics on longer timescales.

[117] Other methods will need to be developed for incorporation of the cross-linker into larger proteins.

[118] The stability of peptide **5** during repeated photolysis was checked by absorbance spectroscopy and HPLC and no indications for sample degradation were observed even after extensive measurements. In particular, no cross-linking between different peptides (nongeminate recombination) occurred under the conditions employed.

[119] Recombination of thiyl radical pairs could be prevented by the addition of external radical quenchers in sufficient concentration. However, such an approach results in irreversible bond dissociation, precluding multiple excitation and thus ruling out the extensive data averaging needed for most of the currently available detection techniques.

[120] G. Jeschke, M. Wakasa, Y. Sakaguchi, H. Hayashi, *J. Phys. Chem.* **1994**, *98*, 4069−4075.

[121] T. Autrey, C. Devadoss, B. Sauerwein, J. A. Franz, G. B. Schuster, *J. Phys. Chem.* **1995**, *99*, 869−871.

[122] J. R. Kumita, O. S. Smart, G. A. Woolley, *Proc. Natl. Acad. Sci. USA* **2000**, *97*, 3803−3808.

[123] R. Behrendt, C. Renner, M. Schenk, F. Wang, J. Wachtveitl, D. Oesterhelt, L. Moroder, *Angew. Chem. Int. Ed.* **1999**, *38*, 2771−2774.

[124] L. Ulysse, J. Cubillos, J. Chmielewski, *J. Am. Chem. Soc.* **1995**, *117*, 8466−8467.

[125] J. Wachtveitl, T. Nägele, B. Puell, W. Zinth, M. Krüger, S. Rudolph-Böhner, D. Oesterhelt, L. Moroder, *J. Photochem. Photobiol. A* **1997**, *105*, 283−288.

[126] R. Cerpa, F. E. Cohen, I. D. Kuntz, *Folding Design* **1996**, *1*, 91−101.

Received September 6, 2000
[O00460]